ACS OMEGA

Open Access

http://pubs.acs.org/journal/acsodf

Article

Application of Nanohybrid Substrates with Layer-by-Layer Self-Assembling Properties to High-Sensitivity Surface-Enhanced Raman Scattering Detection

Published as part of ACS Omega virtual special issue "Celebrating 50 Years of Surface Enhanced Spectroscopy".

Yan-Feng Chen,[†] Yen-Chen Lee,[†] Wen-Wei Lin, Ming-Chang Lu, Yung-Chi Yang, and Chih-Wei Chiu*

Cite This: *ACS Omega* 2024, 9, 1894−1903

Read Online

ACCESS | Metrics & More | Article Recommendations | Supporting Information

ABSTRACT: The present study was conducted to prepare and investigate large-area, high-sensitivity surface-enhanced Raman scattering (SERS) substrates. Organic/inorganic nanohybrid dispersants consisting of an amphiphilic triblock copolymer (hereafter referred to simply as "copolymer") and graphene oxide (GO) were used to stabilize the growth and size of gold nanoparticles (AuNPs). Ion−dipole forces were present between the AuNPs and copolymer dispersants, while the hydrogen bonds between GO and the copolymer prevented the aggregation of GO, thereby stabilizing the AuNP/GO nanohybrids. Transmission electron microscopy (TEM) revealed that the AuNPs had particle sizes of 25−35 nm and a relatively uniform size distribution. The AuNP/GO nanohybrids were deposited onto the glass substrate by using the solution drop-casting method and employed for SERS detection. The self-assembling properties of two-dimensional sheet-like GO led to a regular lamellar arrangement of AuNP/GO nanohybrids, which could be used for the preparation of large-area SERS substrates. Following removal of the copolymer by annealing at 300 °C for 2 h, measurements were obtained under scanning electron microscopy. The results confirmed that 2D GO nanosheets were capable of stabilizing AuNPs, with the final size reaching approximately 40 nm. These AuNPs were adsorbed on both sides of the GO nanosheets. Because the GO nanosheets were merely 5 nm-thick, a good three-dimensional hot-junction effect was generated along the *z*-axis of the AuNPs. Lastly, the prepared material was used for the SERS detection of rhodamine 6G (R6G), a commonly used highly fluorescent dye. An enhancement factor (EF) of up to 3.5×10^6 was achieved, and the limit of detection was approximately 10^{-10} M. Detection limits of 10^{-10} M and < 10^{-10} M were also observed with the detection of Direct Blue 200 and the biological molecule adenine. It is therefore evident that AuNP/copolymer/GO nanohybrids are large-area flexible SERS substrates that hold great potential in environmental monitoring and biological system detection applications.

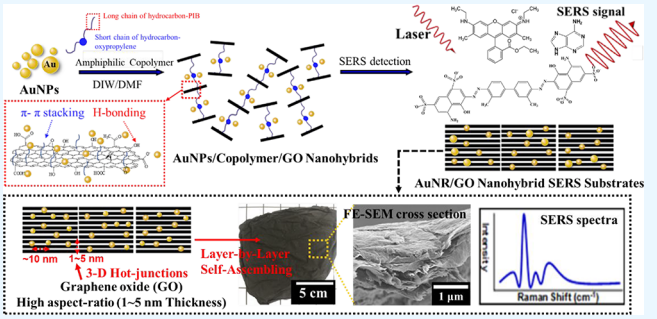

1. INTRODUCTION

Surface-enhanced Raman scattering (SERS) is a promising analytical technique that has rapidly developed because of extensive research,[1−3] having been employed for molecular detection, quantitative analysis,[4,5] and rapid biomedical testing.[6−8] The localized surface plasmon resonance (LSPR) generated by most noble metals − including gold,[9] silver,[10] and copper[11] − has demonstrated superior effects on the enhancement of SERS signals.[12] Although silver has exhibited the most pronounced enhancement effect,[13] the instability of silver nanoparticles during long-term storage and high antibacterial activity have limited their applications.[14] In contrast, gold has high chemical stability, making it extremely useful in chemical synthesis and manufacturing.[15] Recently, researchers have begun to explore the use of gold nanoparticles (AuNPs) in SERS substrates.[16−18] The favorable properties of AuNPs, such as low toxicity and high biocompatibility,[19] have facilitated their widespread application in SERS detection.[20] However, the chemical synthesis method poses certain challenges for the control of stable nanoparticle growth. Therefore, the present study was conducted to design a novel type of nanohybrid material to address the issues of high aggregation tendency and instability in nanoparticles.

In the fields of nanotechnology and materials science, organic/inorganic hybrids are regarded as some of the most important materials of the 21st century.[21−23] Many recent studies have explored the combination of metal nanoparticles

Received: October 31, 2023
Revised: November 26, 2023
Accepted: December 12, 2023
Published: December 26, 2023

with other organic/inorganic nanomaterials to improve SERS signals.[24,25] Common materials can be classified accordingly to form into sphere-like materials such as SiO_2[26] and Fe_2O_3,[27] thread-like materials such as carbon nanotubes (CNTs)[28] and polyvinyl alcohol (PVA) nanofibers,[29] and sheet-like materials such as nanoclays[30] and graphene.[31] The use of nanohybrids increases the dispersibility of nanoparticles, as well as the electric field strength between metal particles. In the present study, graphene oxide (GO) was used as a substrate to enhance the SERS signals of the analyte molecules. GO is a 2D planar material composed of sp^2-hybridized carbon atoms arranged in a hexagonal honeycomb lattice, with the thickness of a single layer being 1−5 nm. When hot-junctions are generated following the adsorption of metal particles onto one side of GO, the hot-junction effect along the longitudinal axis is not blocked by GO. The self-assembling properties of GO also cause the generation of a good three-dimensional hot-junction effect along the *z*-axis by the metal particles.[32] The hot-junction effect, a theory commonly employed in the enhancement of Raman signals, is often used to explain the influence of distance between metal nanoparticles on SERS enhancement.[33] Specifically, the SERS signal intensity is considered to increase with a decrease in interparticle distance. However, the enhancement effects of rough noble metal surfaces and noble metal nanoparticles are often exerted in a unidimensional fashion. Based on the extreme thinness of GO, the interparticle distance of AuNPs was controlled within a range of 1−5 nm. Simultaneously, the self-assembling properties of GO were harnessed to achieve the adsorption of AuNPs on both sides of the GO, generating a 3D hot-junction effect. Molecules of analytes can also be adsorbed onto aromatic rings on the surfaces of GO by $\pi-\pi$ stacking,[34,35] thereby increasing the stability of molecular structures to achieve immense improvement of SERS signals.

In this study, we report the preparation of large-area, flexible, and high-sensitivity SERS substrates. Organic/inorganic nanohybrids − which demonstrated superior properties and a certain level of sensitivity in SERS detection after being developed in our previous work − served as the bases for SERS substrates.[36−38] An amphiphilic triblock copolymer with excellent dispersibility and applicability was also developed in this study.[39,40] However, the presence of strong sp^2-hybridized bonds in the 2D hexagonal honeycomb lattice of GO poses a considerable challenge to the production of stable AuNP/copolymer/GO nanohybrids. We first stabilized the growth of AuNPs and enhanced their dispersibility by using a PIB−ED−PIB copolymer. Subsequently, the AuNP/copolymer was dispersed in inorganic 2D GO, and different weight ratios were assigned to determine the optimal ratio for the AuNP/copolymer/GO nanohybrids. The copolymer was then removed by heat treatment to increase the sensitivity of the SERS signals. Lastly, the prepared material was used for the SERS detection of rhodamine 6G (R6G), Direct Blue 200, and adenine. These large-area, flexible, and low-cost AuNP/copolymer/GO nanohybrids may potentially possess broad applicability when used as SERS substrates.

2. EXPERIMENTAL SECTION

2.1. Materials. The following materials and reagents were used in the present study: graphene oxide (GO, oxygen content of approximately 40%; E WAY Technology Co. (Taiwan)), tetrachloroauric acid (99.9% purity; Echo Chemical Co. (Taiwan)), polyisobutylene-g-succinic anhydride (PIB−SA, Mw = 1,335; Chevron Corp.), poly(oxyethylene)-diamine (POE−diamine or POE-ED2003, Mw = 2,000; Huntsman Chemical Co. (USA)); dimethylformamide (DMF) and rhodamine 6G (R6G) (Echo Chemical Co. (Taiwan)); Direct Blue 200 (Nippon Kayaku Co. (Tokyo, Japan)), adenine ($C_5H_5N_5$, 99.9% purity; Sigma-Aldrich Chemical Co., USA).

2.2. Preparation of AuNP/Copolymer/GO Nanohybrids. Using DMF as the reducing agent, tetrachloroauric acid was reduced to stable AuNPs with the addition of an amphiphilic triblock copolymer (PIB−ED−PIB).[41] First, 0.1 g of $HAuCl_4$ powder was dissolved in 10 mL of deionized water (DIW) and slowly added dropwise into the copolymer solution prepared according to a previously described method,[42] with the DIW/DMF solvent weight ratio controlled at 2/1. The mixture was maintained at 80 °C and stirred continuously for several hours. Color changes in the mixture were observed, and microscopic images were examined by ultraviolet−visible-light (UV−vis) spectroscopy and transmission electron microscopy (TEM). For the preparation of AuNPs/copolymer/GO nanohybrids, GO powder and the copolymer were dispersed in a DIW/DMF solvent at a weight ratio of 2/1 and ultrasonicated for 10 min. AuNP/copolymer/GO nanohybrids of different weight ratios prepared using the one-step synthesis method were separately stirred with a magnetic stirrer at 80 °C for 4 h, and a color change from light yellow to pink was observed. However, the solution color became darker with an increase in the weight ratio of GO. The strongest absorption peak of the nanohybrids was measured by UV−vis spectroscopy to confirm the reduction of Au^{3+} to Au^0. Characteristic peaks of surface plasmon resonance (SPR) were observed in the synthesized nanohybrids, and microscopic images were examined by TEM.

2.3. Preparation of Large-Area SERS Substrates. AuNP/copolymer/GO nanohybrids were poured into a glass Petri dish and allowed to self-assemble into a large-area SERS substrate at room temperature. The lamellar structure of the resultant substrate was examined by field emission scanning electron microscopy (FESEM). Subsequently, the substrate was sintered at 300 °C for 2 h to remove the copolymer and used for SERS detection of three analytes: R6G, Direct Blue 200 (10 μL), and adenine (10 μL). Molecules of each analyte were separately added dropwise to an SERS substrate and allowed to dry. Differences in Raman signals were compared between nanohybrids with different weight ratios, as well as between pre- and postannealed nanohybrids. The prepared concentrations and observed wavelengths (characteristic peaks) of the three analytes were as follows: R6G: 10^{-4}−10^{-10} M, 613 cm^{-1} and 774 cm^{-1}; Direct Blue 200: 10^{-3}−10^{-11} M, 590 cm^{-1} and 1320 cm^{-1}; adenine: 10^{-4}−10^{-11} M, 733 cm^{-1}.

2.4. Characterization and Instruments. UV−vis spectrometry was performed on a Shimadzu UV-2450 spectrophotometer (Kyoto, Japan). The synthesized AuNP/copolymer and AuNP/copolymer/GO nanohybrid suspensions were diluted with DIW at a ratio of 1:1, and absorption at specific wavelengths in the UV−vis spectrum was observed to identify the reduction reaction of the AuNPs. TEM was performed by using a Zeiss EM 902A transmission electron microscope (Tokyo, Japan). 10 μL of the AuNPs/copolymer and AuNPs/copolymer/GO nanohybrid suspensions was separately added dropwise to a carbon-coated copper grid and dried at 80 °C for at least 24 h before TEM imaging. Samples were subjected to

https://doi.org/10.1021/acsomega.3c08608
ACS Omega 2024, 9, 1894−1903

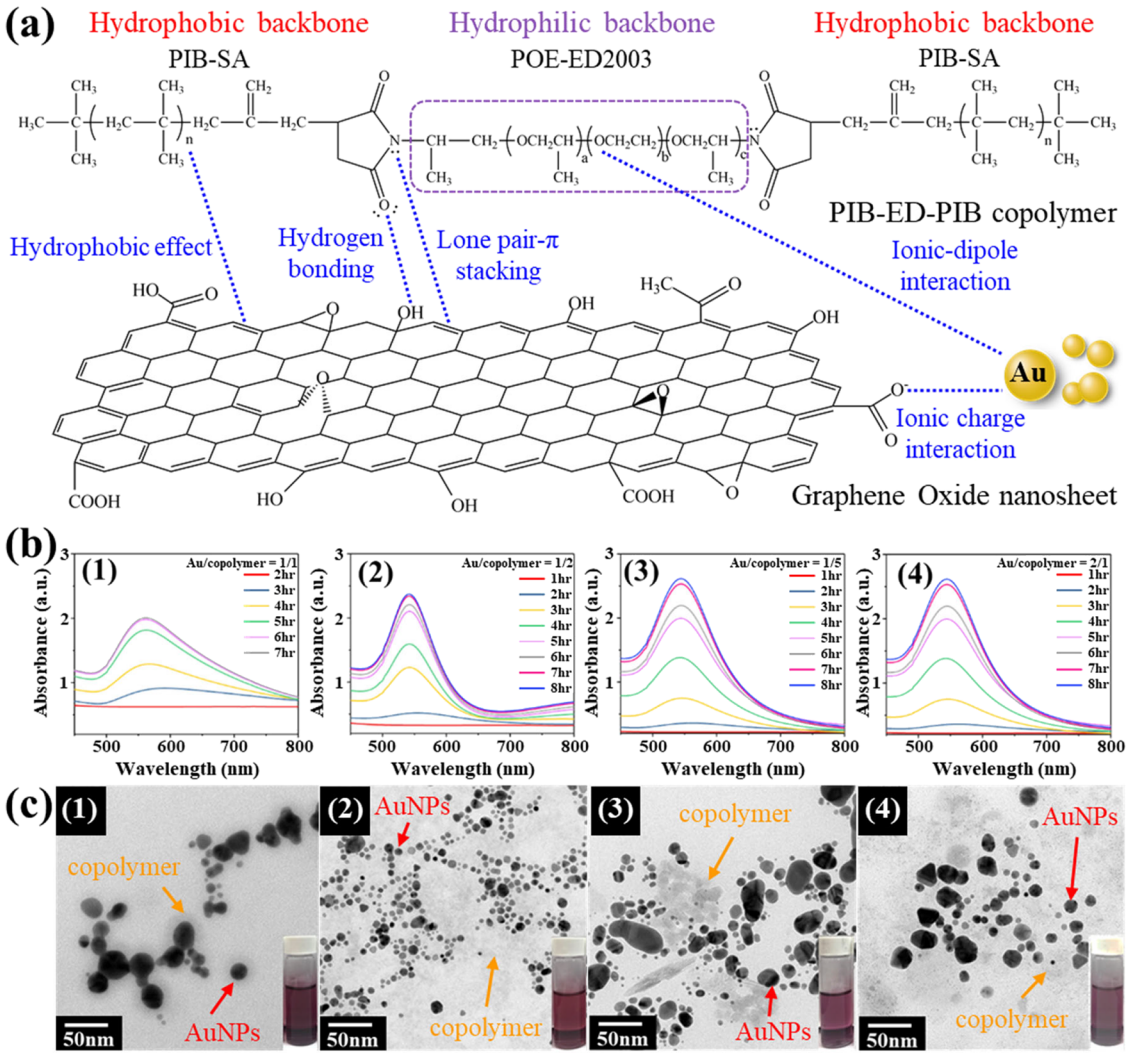

Figure 1. (a) Schematic of the dispersion mechanism in AuNP/copolymer/GO nanohybrids. Dispersion was primarily caused by noncovalent intermolecular interactions − such as ion−dipole interactions, lone pair−π stacking interactions, hydrophobic interactions, and hydrogen bonds − which prevented the aggregation of GO and stabilized the AuNPs; (b) UV−vis spectra of AuNP/copolymer nanohybrids synthesized using different weight ratios: (1) 1/1, (2) 1/2, (3) 1/5, and (4) 2/1; (c) TEM images of AuNP/copolymer nanohybrids synthesized using different weight ratios: (1) 1/1, (2) 1/2, (3) 1/5, and (4) 2/1. Insets: photographs of corresponding AuNP/copolymer solution samples.

high-resolution FESEM using a Zeiss EM 902A system (Tokyo, Japan). The sample to be tested was mounted onto conductive carbon tape and coated with a thin layer of platinum (Pt) for FESEM imaging. Thermogravimetric analysis (TGA) was performed using the TA Instruments Q-500 thermogravimetric analyzer (New Castle, DE, USA), with measurements made by heating from 100 to 700 °C at a heating rate of 10 °C/min under airflow conditions. An X-ray photoelectron spectroscopy (XPS) analysis was carried out with a Thermo Fisher Scientific (VGS) spectrometer (Waltham, MA, USA). Using the Al Kα anode as the X-ray source (1486.6 eV), a binding energy range of 0−1400 eV was selected for analysis. Samples were subjected to micro-Raman spectroscopy using a HORIBA iHR550 spectrometer (Protrustech Corp., Ltd., Tainan, Taiwan). 633-nm laser light was used as the excitation source, with the exposure time and power being 10 s and 20 mW, respectively. The excitation light was focused on an area of approximately 4 μm^2 using a 50× objective lens.

3. RESULTS AND DISCUSSION

3.1. Dispersion Mechanism, Preparation, and Structural Identification of AuNP/Copolymer/GO Nanohybrids. GO is a 2D sheet-like material composed of carbon atoms bonded by covalent bonds, with an oxygen content of approximately 40%. A large number of epoxy functional groups, hydroxyl groups, and carboxyl groups are present on the edges and surfaces of the GO sheets. The GO used in the present study was examined by FESEM (see Figure S1 of Supporting Information), TEM (see Figure S2 of Supporting Information), and Raman spectroscopy (see Figure S3 of Supporting Information). In the Raman spectrum shown in Figure S3 of the Supporting Information, the D-band and G-band peaks of GO are, respectively, located at 1330 and 1600 cm^{-1}, with the D-band-to-G-band intensity ratio (I_D/I_G) being 1.16. These measurements indicate the presence of many defects on the surface structure of GO, which can be regarded as oxygen-containing functional groups. GO is composed of benzene ring structures bonded with other functional groups that are surrounded by a large number of delocalized electrons.

https://doi.org/10.1021/acsomega.3c08608
ACS Omega 2024, 9, 1894−1903

Previous studies have reported that vibrations of delocalized electrons contribute to the enhancement of Raman scattering signals.[43−45] The main forces of attraction between AuNPs and the copolymer were ion−dipole interactions, which enabled the stable growth of AuNPs. Between GO and the copolymer, certain noncovalent bonds − such as lone pair−π stacking interactions, hydrophobic interactions, and hydrogen bonds, were present, preventing the aggregation of GO. Figure 1a illustrates a schematic of the interactions present in the AuNP/copolymer/GO nanohybrids. The copolymer served as a key link between GO and the AuNPs. Hydrophobic PIB blocks on both ends of the copolymer possessed polar carbon rings that interacted with the benzene rings of GO, while the central hydrophilic POE-ED2003 block contributed substantial ion-charge interactions, leading to the close proximity of carbonyl groups on AuNPs and both sides of the GO sheet and giving rise to van der Waals and ionic charge interaction forces that provided further stabilizing effects. Subsequently, the AuNP/copolymer/GO nanohybrid system was investigated in two aspects. First, the effects of different AuNP/copolymer weight ratios (1/1, 1/2, 1/5, and 2/1) were examined. Figure 1b shows the UV−vis absorption spectra to determine the completion of the synthesis reaction under the different weight ratios. It can be observed that a lower copolymer content led to greater instability in the absorption spectrum generated by the AuNPs. Figure 1c presents TEM images indicating the particle size and distribution of AuNP/copolymer nanohybrids synthesized by using different weight ratios. At a weight ratio of 1/1, a certain degree of AuNP aggregation was observed (Figure 1c-(1)), as the copolymer content was insufficient for the stabilization of AuNPs. The same phenomenon was also observed at a weight ratio of 2/1, as shown in Figure 1c-(4). Our TEM images also reveal an evident increase in the average size of AuNPs and different shapes formed from precipitation (see Table S4 of the Supporting Information). However, at a weight ratio of 1/2, the AuNPs exhibited an average particle size of 27 nm under the microscope and a narrow distribution at the maximum absorption peak at 528 nm in the UV−vis spectrum. This finding demonstrates that addition of the copolymer protected the AuNPs and prevented their aggregation. Meanwhile, the low-magnification TEM image in Figure S4 of the Supporting Information shows that the AuNPs/copolymer at a ratio of 1/2 exhibit excellent dispersion. Ultimately, the optimal AuNPs/copolymer weight ratio of 1/2 was selected for further experimentation.

Different weight ratios of AuNP/copolymer/GO nanohybrids were subsequently investigated based on the experimental results described above, as shown in Table 1.

Table 1. Reduction of AuNPs with Different Amounts of Copolymer/Graphene Oxide (GO)

AuNPs/copolymer/GO (weight ratio)	solution Color	zeta potential (mV)	UV−vis absorption (nm)	before annealing particle size (nm)	after annealing particle size (nm)
10/20/1	scarlet	4.1	533	32.1	63.2
5/10/1	pink	3.7	530	21.3	47.9
2/4/1	pink	1.8	534	42.0	52.3
1/2/1	wine	0.9	544	35.1	68.2
1/2/2	wine	0.1	557	40.1	51.4
1/2/5	black	−2	557	33.3	61.0

The zeta potential of pristine GO was −5.4 mV, whereas the zeta potential of AuNPs obtained by reduction with DMF/DIW was 0.9−4.1 mV. These results indicate that in addition to the copolymer, the zeta potential of GO may also serve as a stabilizing agent. The changes in zeta potential also indirectly demonstrate the stable adsorption of AuNPs on the surfaces of GO. Figure 2a shows the absorption spectrum of AuNP/copolymer/GO at a weight ratio of 5/10/1, with the absorption peak located at 530 nm and a reaction time of 6 h. The TEM images shown in Figure 2b reveal that AuNPs possessed a smaller size distribution and uniform shape on the surfaces of GO, with the average particle size being approximately 30 nm. The AuNPs also exhibited a greater tendency to aggregate when a lower GO content was present. The wavelength values of the UV−vis absorption peak, listed in Table 1, indicate that an increase in the weight ratio of GO was associated with a significant red shift in absorbance. Therefore, controlling the AuNP/copolymer/GO weight ratio is key to modifying the dispersion of AuNPs on the GO surfaces and the polymer chain. The AuNP/copolymer/GO weight ratio of 5/10/1 exhibited the optimal dispersion and aggregation properties and was accordingly selected for subsequent experimentation. When used as Raman substrates, AuNP/copolymer/GO nanohybrids can enable the binding of hydrate model molecules onto the surfaces of GO through $\pi-\pi$-stacking and hydrogen bonding. Subsequently, the electron charge transfer between graphene and AuNPs increases the Raman intensity and LSPR. In addition, the high aspect ratio of GO, with a plane area of 100−300 nm and thickness of merely 5 nm, favors the preparation of large-area, flexible SERS substrates. Upon the complete removal of solvent in the AuNP/copolymer/GO solution by evaporation at 50 °C, GO exhibited self-assembling properties, as shown by the schematic diagram in Figure 2c. At low concentrations, GO is capable of moving randomly within a solution. However, the solvent evaporation process restricted the range of movement of GO. When the solvent was completely removed, GO tended to deposit onto the base of the substrate scaffold, forming a dense thin-film structure (Figure 2d). In Figure S5 of the Supporting Information, it is clearly visible that AuNPs are evenly attached to the surface of GO. This allowed the AuNPs to stably exist within the spaces of the 3D structure and created more 3D hot-junctions on both sides of GO, thereby enhancing SERS signal strength. With this simple templating method, substrates with regular structures can be easily fabricated, and SERS substrates of different shapes and sizes can be prepared using different containers.

3.2. Preparation of AuNP/GO Nanohybrid SERS Substrates. SERS performance is dependent on the strength of the electromagnetic field on the surfaces of noble metal particles, as well as chemical interactions between the analyte and SERS substrate.[37−39] Although GO is believed to enhance SERS signal intensity through chemical effects, the contribution of chemical effects to signal enhancement is usually only 10−10^3-fold.[46−48] Compared with that provided by the electromagnetic effect, the enhancement factor provided by the 3D hot-junction effects of AuNP/copolymer/GO may be as high as 10^4−10^7. However, in the AuNP/copolymer/GO system, the copolymer is used for the prevention and control of aggregation. Although this enhances the stability of AuNPs, it also decreases the corresponding electromagnetic enhancement effect. This phenomenon also reduces free electron vibrations in AuNPs at a laser wavelength of 633 nm and

https://doi.org/10.1021/acsomega.3c08608
ACS Omega 2024, 9, 1894−1903

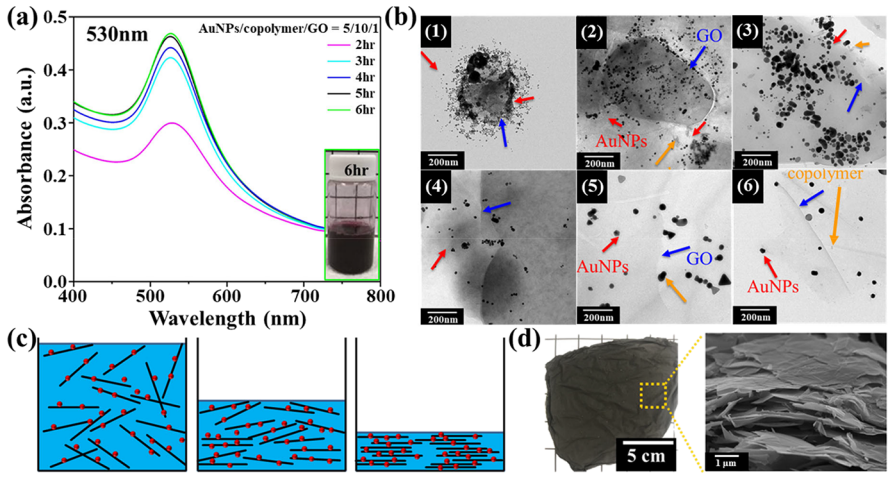

Figure 2. (a) UV−vis spectra showing absorption peak data collected every minute during the reduction process for AuNP/copolymer/GO at a weight ratio of 5/10/1; (b) TEM images showing the morphology and distribution of AuNPs and GO at different AuNP/copolymer/GO weight ratios: (1) 10/20/1, (2) 5/10/1, (3) 2/4/1, (4) 1/2/1, (5) 1/2/1, and (6) 1/2/5; (c) schematic representation of the formation of a thin film-like structure of nanohybrids through their layer-by-layer self-assembling properties as a result of solvent evaporation in the AuNPs/copolymer/GO nanohybrid dispersion liquid; (d) 2D sheet-like characteristics of GO in nanohybrids can be utilized for deposition to the base of the substrate scaffold followed by stacking to form a dense thin-film structure. The cross-sectional SEM image indicates a distinct stacked lamellar structure.

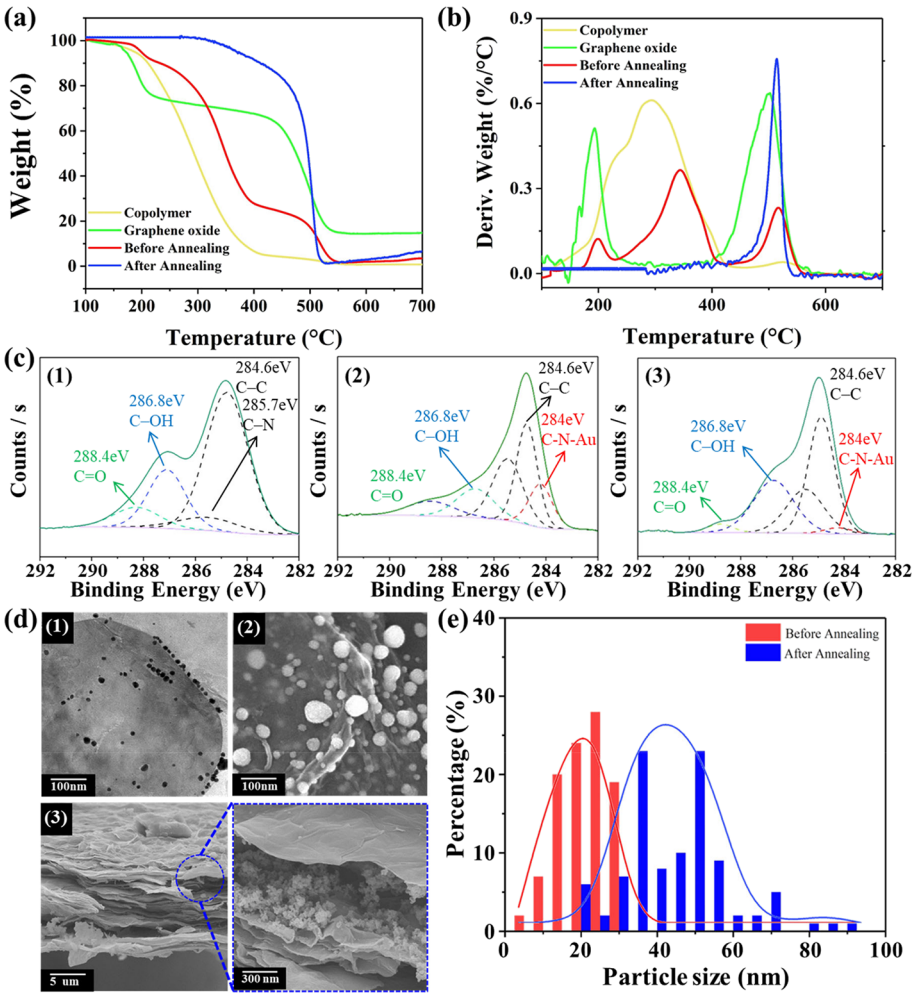

Figure 3. (a) TGA and (b) DTG curves of the copolymer, GO, and pre- and postannealed AuNP/copolymer/GO nanohybrids for the observation of thermal degradation; (c) XPS spectra of AuNP/copolymer/GO substrates: (1) pure GO; (2) preannealed AuNP/copolymer/GO nanohybrids; (3) postannealed AuNP/copolymer/GO nanohybrids; (d) (1) preannealing TEM image for observation of average particle size of AuNPs; (2) postannealing SEM image, indicating that annealing in a high-temperature furnace caused an increase in the particle size of AuNPs; (3) postannealing cross-sectional SEM image; (e) pre- and postannealing particle size distributions.

https://doi.org/10.1021/acsomega.3c08608
ACS Omega 2024, 9, 1894−1903

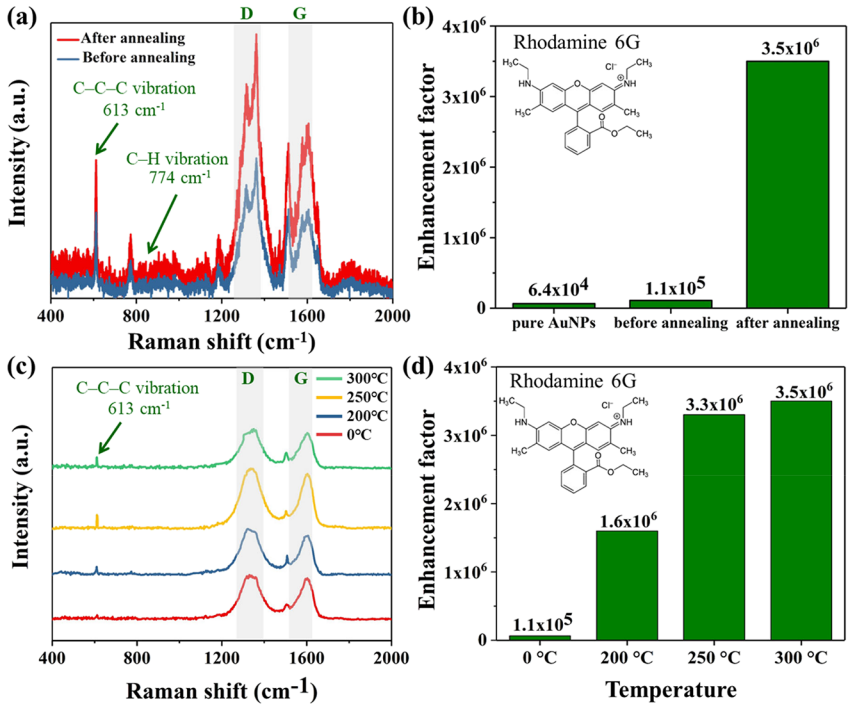

Figure 4. (a) SERS spectra of 10^{-5} M R6G separately obtained using pre- and postannealed AuNP/copolymer/GO with a weight ratio of 5/10/1 as the SERS substrate; (b) comparison of EF values calculated for R6G characteristic peak at 613 cm^{-1}; (c) SERS detection of 10^{-6}M R6G solution under different annealing temperatures; (d) comparison of EF values calculated for the R6G characteristic peak at 613 cm^{-1} under different annealing temperatures.

simultaneously decreases the intensity of the Raman signals. Therefore, the elimination of the copolymer's effects upon obtaining a stable lamellar structure is a critical issue in the preparation of high-sensitivity Raman substrates. Figure 3a presents TGA results of thermal degradation in the copolymer, GO, and AuNP/copolymer/GO. The copolymer began losing weight at approximately 200 °C, with the maximum weight loss rate observed at 295 °C on the derivative thermogravimetry (DTG) curve shown in Figure 3b. The TGA curve of AuNP/copolymer/GO indicates the occurrence of two-step thermal degradation at 300 and 432 °C. Heat treatment was subsequently applied at 300 °C to remove the copolymer from the AuNP/copolymer/GO film prepared with a weight ratio of 5/10/1. An XPS analysis was then conducted to confirm changes in bonding for pure GO and AuNP/copolymer/GO, as shown in Figure 3c. The full range spectra indicate the formation of AuNPs at 84−88 eV. In pure GO, C and O were located at 284 and 560 eV with atomic percentages of 73% and 26%, respectively. The incorporation of AuNPs into GO led to an increase in the oxygen content to 31.8%. After annealing, the aliphatic bonds of POE decreased to 0%, and the relative atomic percentage was 95.1%. The C1s XPS spectra were fitted to different functional groups corresponding to the different peak values of C atoms, with the nonoxidative C−C bond located at 284.6 eV, C−N bond located at 285.7 eV, and C−OH and C═O bonds located at 286.8 eV. The peaks at 286.8 and 288.4 eV in the spectrum for GO indicate the presence of many atomic defects (e.g., C═O, C−OH). Upon the addition of AuNPs and the copolymer, the intensity of the C−N peak was significantly increased, and a peak corresponding to the Au−N−C bond appeared at 284 eV (Figure 3c-(2)). Peak values for C−N and Au−N−C were reduced following the removal of the copolymer. This indicates a decrease in valence-bond interactions, which affected free electron vibrations and effectively enhanced the SERS intensity. When the thermal degradation temperature was within the range of approximately 250−300 °C, the removal of the copolymer by heat treatment in a high-temperature furnace was associated with an increase in the size of AuNPs. However, lamellar stacking in the GO restricted the movement of AuNPs and exerted control of their particle size. AuNP/copolymer/GO at a weight ratio of 5/10/1 was subjected to annealing at 350 °C for 30 min, cooled slowly, and examined by TEM and SEM, as shown in Figure 3d, revealing that the average particle size of AuNPs increased from 21.3 to 47.9 nm (Figure 3e). Table 1 lists the detailed changes in the particle size. A possible explanation is that some of the AuNPs were transformed into a molten state at 350 °C, and the remaining AuNPs underwent a certain extent of growth during the slow cooling process owing to the self-assembling properties of GO.

3.3. Molecular Detection and Applications of AuNP/GO Nanohybrid SERS Substrates. The enhancement effect of AuNP/copolymer/GO nanohybrids on SERS was further assessed using R6G as an analyte. R6G molecules were dissolved in an ethanol solution to a concentration of 10^{-3}−10^{-10} M, and 10 μL of the aqueous solution was added dropwise onto the AuNP/copolymer/GO nanohybrid SERS substrate and allowed to dry at room temperature. In general, the SERS signals of R6G are generated by specific chemical bond vibrations, with the peaks at 613 and 774 cm^{-1} attributed to C−C−C and C−H vibrations, respectively.[49−51] However, the Raman signals of GO at 1330 and 1600 cm^{-1}, which, respectively, belong to the D and G bands, overlap with certain signals of the R6G molecules. Figure 4a depicts a comparison of SERS spectra for 10^{-5} M R6G obtained with pre- and postannealed AuNP/copolymer/GO, indicating that the

https://doi.org/10.1021/acsomega.3c08608
ACS Omega 2024, 9, 1894−1903

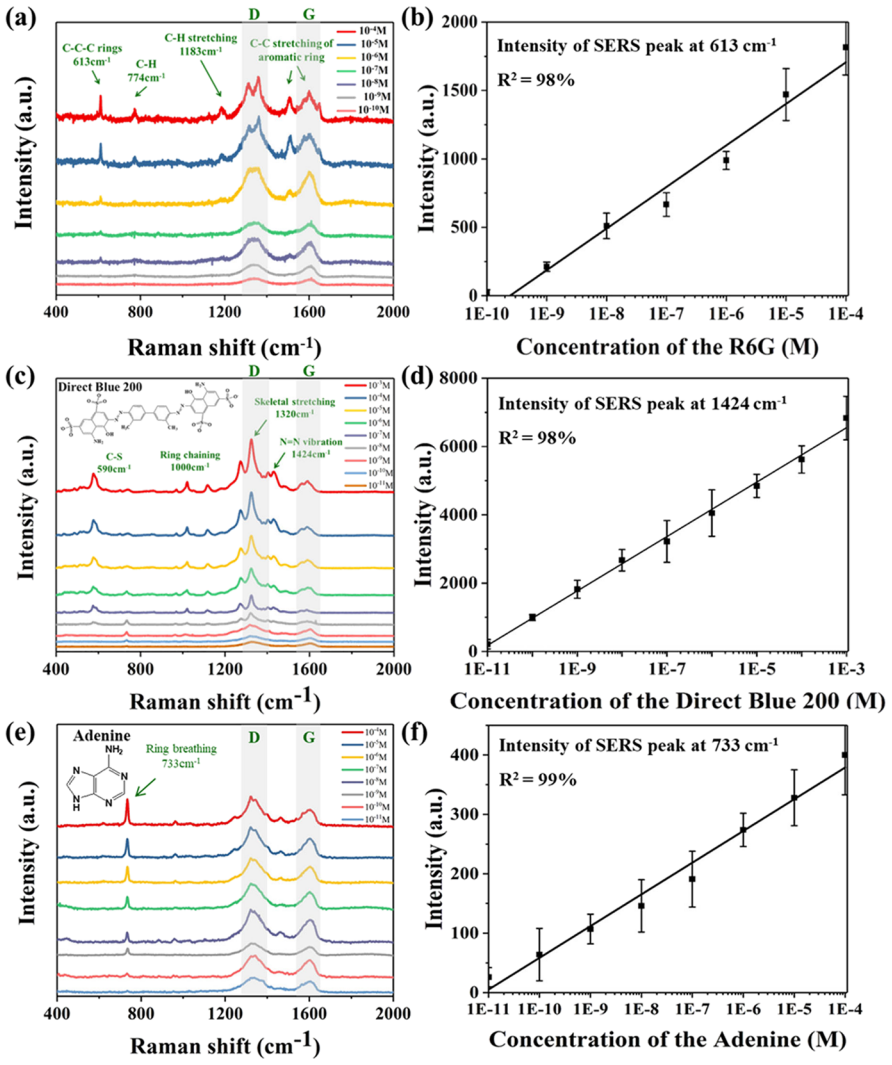

Figure 5. SERS detection using postannealed AuNPs/GO nanohybrid substrate with a weight ratio of 5/10/1 (AuNPs/copolymer/GO): (a) SERS detection limits for R6G at different concentrations; (b) linear regression of intensities of R6G characteristic peak at 613 cm^{-1}; (c) SERS detection limits for Direct Blue 200 at different concentrations; (d) linear regression of intensities of Direct Blue 200 characteristic peak at 1424 cm^{-1}; (e) SERS detection limits for adenine at different concentrations; (f) linear regression of intensities of adenine characteristic peak at 733 cm^{-1}.

postannealed SERS substrate led to an approximately 3-fold increase in signal intensity. The enhancement factor (EF) was calculated using the following formula:[36−39]

$$EF = (I_{SERS}/N_{SERS})/(I_{ref}/N_{ref})$$

where I_{SERS} and I_{ref} are the integration of the signals of R6G at 613 cm^{-1} on glass and substrate, respectively, and N_{SERS} and N_{ref} are the corresponding detected concentrations of R6G. The EF achieved with AuNP/copolymer/GO annealed at 300 °C was 3.5×10^6 (Figure 4b). Figure 4c,d shows the effects of different annealing temperatures on the detection results of R6G. It can be seen that EF values of 3.3×10^6 and 1.6×10^6 could also be achieved at temperatures of 200 and 250 °C. However, incomplete copolymer degradation resulted in relatively lower SERS signal intensities on the same substrate.

The detection limit for R6G was further investigated to examine the sensitivity of the prepared substrates. As shown in Figure 5a, a detection limit of approximately 10^{-10} M was achieved by the postannealed AuNP/copolymer/GO. R6G characteristic peak intensities at 613 cm^{-1} were arranged in ascending order and subjected to a linear regression analysis. Figure 5b shows that a standard error (R^2) value of 98% can be achieved. To expand the applicability of the prepared AuNPs/copolymer/GO substrate in the field of SERS detection, we also used the substrate for the detection of Direct Blue 200 under laser excitation at a wavelength of 633 nm. As shown in Figure 5c, a detection limit of 10^{-10} M was attained for Direct Blue 200, which adsorbed to the surfaces of GO through N and S atoms. Significant signal enhancements were also observed at 1320 and 1424 cm^{-1}, and a high R^2 value of 98% was obtained via linear regression at 1424 cm^{-1} (Figure 5d). Lastly, we analyzed the biological molecule adenine, a basic component of DNA, which is commonly used to demonstrate the feasibility of biological testing. Figure 5e shows that a detection limit of 10^{-10} M was achieved for adenine, and an R^2 value of 99% was obtained via linear regression at 733 cm^{-1} (Figure 5f). The SERS detection results for the aforementioned analytes jointly demonstrate that the SERS substrate prepared using AuNP/copolymer/GO nanohybrids yields excellent detection performance with characteristics of rapidity and high sensitivity. Typically, environmental and biological analyses are performed in liquid condition.

https://doi.org/10.1021/acsomega.3c08608
ACS Omega 2024, 9, 1894−1903

Conventional SERS substrates often use drop-casting methods for liquid analyte detection, but during the drying process, they tend to induce the coffee ring effect,[52] causing the analytes to concentrate around the edges. Producing AuNPs/GO as thin films effectively mitigates this phenomenon and substantially increases the contact area between analytes and the nanoparticles. Therefore, the potential for broad applications in the field of SERS has been successfully realized.

4. CONCLUSIONS

In the present study, we successfully prepared AuNP/copolymer/GO nanohybrids that demonstrated excellent detection performance and high sensitivity when used as SERS substrates. The AuNP enhanced the stability of the GO through anchoring on both sides of the 2D GO material. The copolymer further facilitated AuNP stabilization and dispersion, and the hydrophilic block at the center and hydrophobic blocks at the ends of the triblock polymer provided a linking effect between the AuNPs and GO. By variation of the weight ratio of the nanohybrids, the optimal parameters were identified for further application to SERS detection. At a AuNP/copolymer/GO weight ratio of 5/10/1, uniform particle sizes and similar particle shapes could be achieved. GO was also observed to assist in increasing the particle sizes of AuNPs to approximately 25 nm, which further increased to 47−58 nm following removal of the copolymer through annealing at 300 °C. The self-assembling behavior of GO contributed to the formation of a lamellar structure in the substrate, thereby generating a 3D hot-junction effect and increasing the intensity of SERS signals. Aside from having a novel lamellar arrangement, the AuNP/copolymer/GO-based SERS substrate can also be easily fabricated through a process that favors the production of large-area substrates. The prepared substrate demonstrated superior performance in the SERS detection of R6G, Direct Blue 200, and adenine. A high EF value of 3×10^6 and detection limit of 10^{-10} M were achieved for R6G detection, and detection limits of 10^{-10} M and $< 10^{-10}$ M were obtained with Direct Blue 200 and adenine, respectively. These findings amply indicate the extremely high detection sensitivity of the AuNP/copolymer/GO nanohybrids. We expect this novel material to serve as an environmentally friendly, low-cost, and mass-producible SERS substrate for the partial replacement of existing SERS substrates that require high precision of detection.

■ ASSOCIATED CONTENT

Supporting Information

The Supporting Information is available free of charge at https://pubs.acs.org/doi/10.1021/acsomega.3c08608.

SEM images of pristine GO powder; TEM images of pristine GO; Raman spectrum of GO; TEM images of AuNPs/copolymer nanohybrids; SEM image of AuNPs/copolymer/GO nanohybrids; UV−vis absorption wavelengths and particle sizes of AuNPs/copolymer nanohybrids (PDF)

■ AUTHOR INFORMATION

Corresponding Author

Chih-Wei Chiu − *Department of Materials Science and Engineering, National Taiwan University of Science and Technology, Taipei 10607, Taiwan;* orcid.org/0000-0003-2258-2454; Phone: +886-2-2737-6521; Email: cwchiu@mail.ntust.edu.tw

Authors

Yan-Feng Chen − *Department of Materials Science and Engineering, National Taiwan University of Science and Technology, Taipei 10607, Taiwan*

Yen-Chen Lee − *Department of Materials Science and Engineering, National Taiwan University of Science and Technology, Taipei 10607, Taiwan*

Wen-Wei Lin − *Department of Materials Science and Engineering, National Taiwan University of Science and Technology, Taipei 10607, Taiwan*

Ming-Chang Lu − *Department of Materials Science and Engineering, National Taiwan University of Science and Technology, Taipei 10607, Taiwan*

Yung-Chi Yang − *Department of Materials Science and Engineering, National Taiwan University of Science and Technology, Taipei 10607, Taiwan*

Complete contact information is available at: https://pubs.acs.org/10.1021/acsomega.3c08608

Author Contributions

†Y.-F.C. and Y.-C.L. contributed equally to this work. The manuscript was written through contributions from all the authors. Data curation, Y.-F.C. and Y.-C.L.; formal analysis, Y.-F.C., Y.-C.L., and W.-W.L.; supervision, C.-W.C.; writing − original draft, Y.-F.C., Y.-C.L., and C.-W.C.; writing − review and editing, Y.-F.C., Y.-C.L., W.-W.L., M.-C.L., Y.-C.Y., and C.-W.C.. All authors have read and agreed to the published version of the manuscript.

Notes

The authors declare no competing financial interest.

■ ACKNOWLEDGMENTS

This research was funded by the National Science and Technology Council (MOST 111-2628-E-011-009-MY3, NSTC 112-2622-8-011-012-TE2, and NSTC 112-2221-E-011-004-MY3) of Taiwan.

■ REFERENCES

(1) Murugappan, S.; Tofail, S. A.; Thorat, N. D. Raman Spectroscopy: A Tool for Molecular Fingerprinting of Brain Cancer. *ACS Omega* **2023**, *8*, 27845−27861.

(2) Tan, Y.; Yang, K.; Zhang, X.; Zhou, Z.; Xu, Y.; Xie, A.; Xue, C. Stretchable and Flexible Micro−Nano Substrates for SERS Detection of Organic Dyes. *ACS Omega* **2023**, *8*, 14541−14548.

(3) Itoh, T.; Procházka, M.; Dong, Z. C.; Ji, W.; Yamamoto, Y. S.; Zhang, Y.; Ozaki, Y. Toward a New Era of SERS and TERS at The Nanometer Scale: From Fundamentals to Innovative Applications. *Chem. Rev.* **2023**, *123*, 1552−1634.

(4) Yang, W.; Tang, J.; Ou, Q.; Yan, X.; Liu, L.; Liu, Y. Recyclable Ag-Deposited TiO_2 SERS Substrate for Ultrasensitive Malachite Green Detection. *ACS Omega* **2021**, *6*, 27271−27278.

(5) Li, H.; Yang, Q.; Hou, J.; Li, Y.; Li, M.; Song, Y. Bioinspired Micropatterned Superhydrophilic Au-Areoles for Surface-Enhanced Raman Scattering (SERS) Trace Detection. *Adv. Funct. Mater.* **2018**, *28*, 1800448.

(6) Zacharovas, E.; Velička, M.; Platkevičius, G.; Čekauskas, A.; Želvys, A.; Niaura, G.; Šablinskas, V. Toward a SERS Diagnostic Tool for Discrimination Between Cancerous and Normal Bladder Tissues via Analysis of The Extracellular Fluid. *ACS Omega* **2022**, *7*, 10539−10549.

(7) Hickey, M. E.; He, L. Understanding and Advancing the 3-Mercaptophenylboronic Acid Chemical Label for Optimal Surface-

Enhanced Raman Spectroscopic Analysis of Bacteria Populations. *ACS Appl. Bio Mater.* **2020**, *3*, 8768−8775.
(8) Chen, Y. F.; Wang, C. H.; Chang, W. R.; Li, J. W.; Hsu, M. F.; Sun, Y. S.; Liu, T. Y.; Chiu, C. W. Hydrophilic−Hydrophobic Nanohybrids of AuNP-Immobilized Two-Dimensional Nanomica Platelets as Flexible Substrates for High-Efficiency and High-Selectivity Surface-Enhanced Raman Scattering Microbe Detection. *ACS Appl. Bio Mater.* **2022**, *5*, 1073−1083.
(9) Lu, Y.; Lei, B.; Zhao, Q.; Yang, X.; Wei, Y.; Xiao, T.; Zhu, S.; Ouyang, Y.; Zhang, H.; Cai, W. Solid-State Au Nanocone Arrays Substrate for Reliable SERS Profiling of Serum for Disease Diagnosis. *ACS Omega* **2023**, *8*, 29836−29846.
(10) Wang, D.; Bao, L.; Li, H.; Guo, X.; Liu, W.; Wang, X.; Hou, X.; He, B. Polydopamine Stabilizes Silver Nanoparticles as a SERS Substrate for Efficient Detection of Myocardial Infarction. *Nanoscale* **2022**, *14*, 6212−6219.
(11) Lu, Y.; Bi, Z.; Shang, G. Facile Method to Fabricate Cactus-like AgNPs/CuO/Cu_2O Nanocomposites for Recyclable SERS Detection of Trace Carbendazim Residues. *ACS Appl. Nano Mater.* **2022**, *5*, 17806−17818.
(12) He, M. Q.; Yu, Y. L.; Wang, J. H. Biomolecule-Tailored Assembly and Morphology of Gold Nanoparticles for LSPR Applications. *Nano Today* **2020**, *35*, No. 101005.
(13) Hsu, Z. H.; Hsu, L.; Huang, C. C. Polyacrylamide Gel Scaffold Immobilized with Silver Nanoparticles as SERS Substrates and Catalysts for H_2 Generation via Methanolysis of $NaBH_4$. *ACS Appl. Nano Mater.* **2022**, *5*, 2258−2265.
(14) Gong, H.; Zhang, K.; Dicko, C.; Bülow, L.; Ye, L. Ag−Polymer Nanocomposites for Capture, Detection, and Destruction of Bacteria. *ACS Appl. Nano Mater.* **2019**, *2*, 1655−1663.
(15) Shao, Y.; Zhu, Y.; Zheng, R.; Wang, P.; Zhao, Z.; An, J. Highly Sensitive and Selective Surface Molecularly Imprinted Polymer Electrochemical Sensor Prepared by Au and MXene Modified Glassy Carbon Electrode for Efficient Detection of Tetrabromobisphenol A in Water. *Adv. Compos. Hybrid Mater.* **2022**, *5*, 3104−3116.
(16) Kapara, A.; Brunton, V.; Graham, D.; Faulds, K. Investigation of Cellular Uptake Mechanism of Functionalised Gold Nanoparticles into Breast Cancer Using SERS. *Chem. Sci.* **2020**, *11*, 5819−5829.
(17) Gushiken, N. K.; Paganoto, G. T.; Temperini, M. L.; Teixeira, F. S.; Salvadori, M. C. Substrate for Surface-Enhanced Raman Spectroscopy Formed by Gold Nanoparticles Buried in Poly(Methyl Methacrylate). *ACS Omega* **2020**, *5*, 10366−10373.
(18) Kang, J. W.; So, P. T.; Dasari, R. R.; Lim, D. K. High Resolution Live Cell Raman Imaging Using Subcellular Organelle-Targeting SERS-Sensitive Gold Nanoparticles with Highly Narrow Intra-Nanogap. *Nano Lett.* **2015**, *15*, 1766−1772.
(19) Sani, A.; Cao, C.; Cui, D. Toxicity of Gold Nanoparticles (AuNPs): A Review. *Biochem. Biophys. Rep.* **2021**, *26*, No. 100991.
(20) Lednický, T.; Bonyár, A. Large Scale Fabrication of Ordered Gold Nanoparticle−Epoxy Surface Nanocomposites and Their Application as Label-Free Plasmonic DNA Biosensors. *ACS Appl. Mater. Interfaces* **2020**, *12*, 4804−4814.
(21) Zhao, N.; Yan, L.; Zhao, X.; Chen, X.; Li, A.; Zheng, D.; Zhou, X.; Dai, X.; Xu, F. J. Versatile Types of Organic/Inorganic Nanohybrids: From Strategic Design to Biomedical Applications. *Chem. Rev.* **2019**, *119*, 1666−1762.
(22) Soong, Y. C.; Chiu, C. W. Multilayered Graphene/Boron Nitride/Thermoplastic Polyurethane Composite Films with High Thermal Conductivity, Stretchability, and Washability for Adjustable-Cooling Smart Clothes. *J. Colloid Interface Sci.* **2021**, *599*, 611−619.
(23) Soong, Y. C.; Li, J. W.; Chen, Y. F.; Chen, J. X.; Sanchez, W. A. L.; Tsai, W. Y.; Chou, T. Y.; Cheng, C. C.; Chiu, C. W. Polymer-Assisted Dispersion of Boron Nitride/Graphene in a Thermoplastic Polyurethane Hybrid for Cooled Smart Clothes. *ACS Omega* **2021**, *6*, 28779−28787.
(24) Demirel, G.; Usta, H.; Yilmaz, M.; Celik, M.; Alidagi, H. A.; Buyukserin, F. Surface-Enhanced Raman Spectroscopy (SERS): An Adventure from Plasmonic Metals to Organic Semiconductors as SERS Platforms. *J. Mater. Chem. C* **2018**, *6*, 5314−5335.
(25) Guselnikova, O.; Lim, H.; Kim, H. J.; Kim, S. H.; Gorbunova, A.; Eguchi, M.; Postnikov, P.; Nakanishi, T.; Asahi, T.; Na, J.; Yamauchi, Y. New Trends in Nanoarchitectured SERS Substrates: Nanospaces, 2D Materials, and Organic Heterostructures. *Small* **2022**, *18*, 2107182.
(26) Guo, S.; Jin, S.; Park, E.; Chen, L.; Mao, Z.; Jung, Y. M. Photo-Induced Charge Transfer Enhancement for SERS in a SiO_2−Ag−Reduced Graphene Oxide System. *ACS Appl. Mater. Interfaces* **2021**, *13*, 5699−5705.
(27) Pramanik, A.; Mayer, J.; Sinha, S. S.; Sharma, P. C.; Patibandla, S.; Gao, Y.; Corby, L. R.; Bates, J. T.; Bierdeman, M. A.; Tandon, R.; Seshadri, R.; Ray, P. C. Human ACE2 Peptide-Attached Plasmonic-Magnetic Heterostructure for Magnetic Separation, Surface Enhanced Raman Spectroscopy Identification, and Inhibition of Different Variants of SARS-CoV-2 Infections. *ACS Appl. Bio Mater.* **2022**, *5*, 4454−4464.
(28) Yang, R.; Zhang, Z.; Miao, N.; Fang, W.; Xiao, Z.; Shen, X.; Xin, W. High-Yield Gold Nanohydrangeas on Three-Dimensional Carbon Nanotube Foams for Surface-Enhanced Raman Scattering Sensors. *ACS Omega* **2023**, *8*, 26973−26981.
(29) Chiu, C. W.; Lin, P. H. Core/Shell Ag@Silicate Nanoplatelets and Poly(vinyl alcohol) Spherical Nanohybrids Fabricated by Coaxial Electrospraying as Highly Sensitive SERS Substrates. *RSC Adv.* **2016**, *6*, 67204−67211.
(30) Lee, Y. C.; Chiu, C. W. Immobilization and 3D Hot-Junction Formation of Gold Nanoparticles on Two-Dimensional Silicate Nanoplatelets as Substrates for High-Efficiency Surface-Enhanced Raman Scattering Detection. *Nanomaterials* **2019**, *9*, 324.
(31) Jiang, L.; Niu, G.; Wu, H.; Zhao, J.; Liu, Y.; Xie, Z.; Yao, Q.; Yu, W.; Ren, W.; Zhao, G. Detection of K562 Leukemia Cells in Different States Using a Graphene-SERS Platform. *ACS Appl. Nano Mater.* **2021**, *4*, 8972−8978.
(32) Chiu, C. W.; Lee, Y. C.; Ou, G. B.; Cheng, C. C. Controllable 3D Hot-junctions of Silver Nanoparticles Stabilized by Amphiphilic Tri-block Copolymer/Graphene Oxide Hybrid Surfactants for Use as Surface-Enhanced Raman Scattering Substrates. *Ind. Eng. Chem. Res.* **2017**, *56*, 2935−2942.
(33) Yockell-Lelièvre, H.; Lussier, F.; Masson, J. F. Influence of The Particle Shape and Density of Self-Assembled Gold Nanoparticle Sensors on LSPR and SERS. *J. Phys. Chem. C* **2015**, *119*, 28577−28585.
(34) Li, J. W.; Huang, C. Y.; Zhou, B. H.; Hsu, M. F.; Chung, S. F.; Lee, W. C.; Tsai, W. Y.; Chiu, C. W. High Stretchability and Conductive Stability of Flexible Hybrid Electronic Materials for Smart Clothing. *Chem. Eng. J. Adv.* **2022**, *12*, No. 100380.
(35) Li, J. W.; Lee, J. C. M.; Chuang, K. C.; Chiu, C. W. Photocured, Highly Flexible, and Stretchable 3D-Printed Graphene/Polymer Nanocomposites for Electrocardiography and Electromyography Smart Clothing. *Prig. Org. Coat.* **2023**, *176*, No. 107378.
(36) Chang, W. R.; Hsiao, C.; Chen, Y. F.; Kuo, C. F. J.; Chiu, C. W. Au Nanorods on Carbon-Based Nanomaterials as Nanohybrid Substrates for High-Efficiency Dynamic Surface-Enhanced Raman Scattering. *ACS Omega* **2022**, *7*, 41815−41826.
(37) Chen, Y. F.; Chang, W. R.; Lee, C. J.; Chiu, C. W. Triangular Gold Nanoplates/Two-Dimensional Nano Mica Platelets with a 3D Lightning-Rod Effect as Flexible Nanohybrid Substrates for SERS Bacterial Detection. *J. Mater. Chem. B* **2022**, *10*, 9974−9983.
(38) Chen, Y. F.; Chang, W. R.; Wang, J. H.; Kuo, C. F. J.; Cheng, C. C.; Chiu, C. W. Triangular Silver Nanoplates/Graphene Oxide Nanohybrids on Flexible Substrates for Detection of Bacteria via Surface-Enhanced Raman Spectroscopy. *ACS Appl. Nano Mater.* **2023**, *6*, 13604−13615.
(39) Huang, C. Y; Chiu, C. W. Facile Fabrication of a Stretchable and Flexible Nanofiber Carbon Film-Sensing Electrode by Electrospinning and Its Application in Smart Clothing for ECG and EMG Monitoring. *ACS Appl. Electron. Mater.* **2021**, *3*, 676−686.
(40) Chiu, C. W.; Huang, C. Y.; Li, J. W.; Li, C. L. Flexible Hybrid Electronics Nanofiber Electrodes with Excellent Stretchability and

https://doi.org/10.1021/acsomega.3c08608
ACS Omega 2024, 9, 1894−1903

Highly Stable Electrical Conductivity for Smart Clothing. *ACS Appl. Mater. Interfaces* **2022**, *14*, 42441−42453.
(41) Li, J. W.; Chen, Y. S.; Chen, Y. F.; Chen, J. X.; Kuo, C. F. J.; Chen, L. Y.; Chiu, C. W. Enhanced Efficiency of Dye-Sensitized Solar Cells Based on Polymer-Assisted Dispersion of Platinum Nanoparticles/Carbon Nanotubes Nanohybrid Films as FTO-Free Counter Electrodes. *Polymers* **2021**, *13*, 3103.
(42) Chiu, C. W.; Li, J. W.; Huang, C. Y.; Yang, S. S.; Soong, Y. C.; Lin, C. L.; Lee, J. C. M.; Sanchez, W. A. L.; Cheng, C. C.; Suen, M. C. Controlling the Structures, Flexibility, Conductivity Stability of Three-Dimensional Conductive Networks of Silver Nanoparticles/Carbon-Based Nanomaterials with Nanodispersion and Their Application in Wearable Electronic Sensors. *Nanomaterials* **2020**, *10*, 1009.
(43) Guan, M.; Zhu, Y.; Yue, X.; Liang, Y.; Sheng, H.; Wang, J.; Zhang, C.; Peng, Q.; Lu, G. Molecular Cocatalyst-Induced Enhancement of the Plasmon-Mediated Coupling of p-Nitrothiophenols at the Silver Nanoparticle−Graphene Oxide Interface. *ACS Appl. Nano Mater.* **2021**, *4*, 10976−10984.
(44) Sheng, S.; Ren, Y.; Yang, S.; Wang, Q.; Sheng, P.; Zhang, X.; Liu, Y. Remarkable SERS Detection by Hybrid Cu_2O/Ag Nanospheres. *ACS Omega* **2020**, *5*, 17703−17714.
(45) Jaitpal, S.; Chavva, S. R.; Mabbott, S. 3D Printed SERS-Active Thin-Film Substrates Used to Quantify Levels of the Genotoxic Isothiazolinone. *ACS Omega* **2022**, *7*, 2850−2860.
(46) Ling, X.; Xie, L.; Fang, Y.; Xu, H.; Zhang, H.; Kong, J.; Dresselhaus, M. S.; Zhang, J.; Liu, Z. Can Graphene be Used as A Substrate for Raman Enhancement? *Nano Lett.* **2010**, *10*, 553−561.
(47) Biroju, R. K.; Marepally, B. C.; Malik, P.; Dhara, S.; Gengan, S.; Maity, D.; Narayanan, T. N.; Giri, P. K. Defective Graphene/Plasmonic Nanoparticle Hybrids for Surface-Enhanced Raman Scattering Sensors. *ACS Omega* **2023**, *8*, 4344−4356.
(48) Lipovka, A.; Fatkullin, M.; Shchadenko, S.; Petrov, I.; Chernova, A.; Plotnikov, E.; Menzelintsev, V.; Li, S.; Qiu, L.; Cheng, C.; Rodriguez, R. D.; Sheremet, E. Textile Electronics with Laser-Induced Graphene/Polymer Hybrid Fibers. *ACS Appl. Mater. Interfaces* **2023**, *15*, 38946−38955.
(49) Nong, J.; Tang, L.; Lan, G.; Luo, P.; Li, Z.; Huang, D.; Shen, J.; Wei, W. Combined Visible Plasmons of Ag Nanoparticles and Infrared Plasmons of Graphene Nanoribbons for High-Performance Surface-Enhanced Raman and Infrared Spectroscopies. *Small* **2021**, *17*, 2004640.
(50) Wu, K.; Lai, K.; Chen, J.; Yao, J.; Zeng, S.; Jiang, T.; Si, H.; Gu, C.; Jiang, J. AgNC and AgNP/PorC Film-Based Surface-Enhanced Raman Spectroscopy-Type Immunoassay for Ultrasensitive Prostate-Specific Antigen Detection. *ACS Omega* **2023**, *8*, 18523−18529.
(51) Sun, Z.; Gao, Y.; Ban, C.; Meng, J.; Wang, J.; Wang, K.; Gan, L. 3 nm-Wide WO_{3-x} Nanorods with Abundant Oxygen Vacancies as Substrates for High-Sensitivity SERS Detection. *ACS Appl. Nano Mater.* **2023**, *6*, 8635−8642.
(52) Chen, R.; Zhang, L.; Li, X.; Ong, L.; Soe, Y. G.; Sinsua, N.; Gras, S. L.; Tabor, R. F.; Wang, X.; Shen, W. Trace Analysis and Chemical Identification on Cellulose Nanofibers-Textured SERS Substrates Using the "Coffee Ring" Effect. *ACS Sens.* **2017**, *2*, 1060−1067.

https://doi.org/10.1021/acsomega.3c08608
ACS Omega 2024, 9, 1894−1903